crystals

MDPI

Review

Inorganic–Organic Hybrid Surfactant Crystals: Structural Aspects and Functions

Takeru Ito

Department of Chemistry, School of Science, Tokai University, 4-1-1 Kitakaname, Hiratsuka 259-1292, Japan; takeito@keyaki.cc.u-tokai.ac.jp; Tel.: +81-463-58-1211 (ext. 3737); Fax: +81-463-50-2094

Academic Editor: Helmut Cölfen
Received: 28 January 2016; Accepted: 7 March 2016; Published: 10 March 2016

Abstract: Hybrid single crystals consisting of an organic surfactant and an inorganic moiety are promising functional materials. Layered crystals composed from alternate inorganic and surfactant layers are obtained by the template effect of long alkyl chain moiety. The composition, crystal packing, and molecular arrangement of the hybrid single crystals are controllable by changing the inorganic constituent and the surfactant molecular structure. The types of hybrid surfactant single crystals are twofold: (i) crystals consisting of discrete inorganic cation coordinated by ligands having amphiphilic moiety; and (ii) crystals comprising a surfactant cation and a discrete inorganic anion including polyoxometalate (POM) oxide clusters. The POM-surfactant hybrid single crystals are rather rare, and therefore promising as unprecedented functional materials. Their structural variation and functional properties are discussed.

Keywords: inorganic–organic; hybrid material; single crystal; surfactant; polyoxometalate

1. Introduction

Construction of functional materials by a bottom-up strategy requires precise structural control of the component species. Small molecular or ionic species of the sub-nanometer order (<1 nm) are built into three-dimensional structures of the nano- or micrometer order. In the construction process, molecular or ionic component structures should be controlled, and an assembling methodology of molecular or ionic components is also quite significant.

A promising option for constructing functional materials is inorganic–organic hybrid materials [1–5]. We can expect synergy of the merits derived from inorganic and organic components. The inorganic motif has wide options to select the consisting elements, and to bring thermal stability and various functions. On the other hand, the organic motif enables easy control of the molecular structure. We can make a flexible and precise design of the materials' structures and functions, which leads to novel functional materials. Among several assembling structures, the layered materials possess a two-dimensional arrangement of constituent ions or molecules. This structural anisotropy is beneficial to functional properties such as electronic or ionic conductivity [6–9]. In addition, two-dimensional confinement of functional ions or molecules will lead to several interesting properties [10–14].

To construct inorganic–organic hybrid layered structures, surfactants or molecules with long alkyl chain(s) can be employed as an organic motif (Figure 1) because they self-assemble into a lamellar structure to behave as a synthetic template [15–17]. As for inorganic motifs, metal ions such as transition metals or lanthanide ions can contribute to the emergence of physicochemical functions such as redox, magnetic, or photoluminescent properties [10–14]. In addition, the introduction of inorganic motifs leads to an increase in melting point and thermal stability. Discrete inorganic ions contained in the hybrid surfactant materials are metal cations coordinated by organic ligands, or inorganic anions of metal halides [13], metal chalcogenides [16], and metal oxides (polyoxometalates, POMs) [18–26].

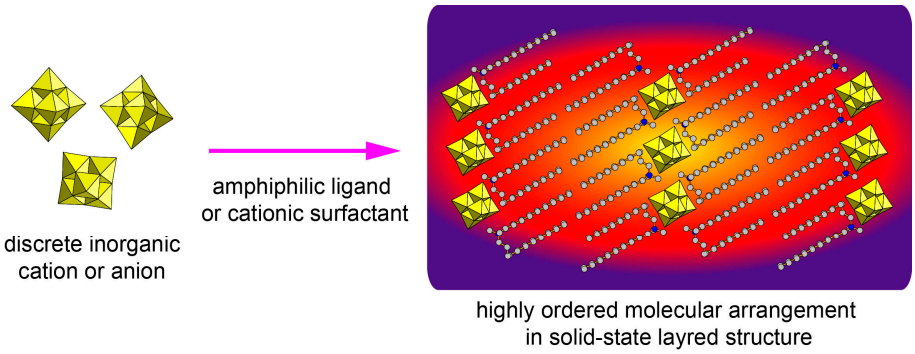

Figure 1. Schematic representation of hybrid surfactant single crystals with layered structures.

Inorganic–organic surfactant layered materials are better for fabricating crystalline materials since the well-ordered two-dimensional arrangement of ions and/or molecules is effective for the emergence of several functions. Crystalline layered materials with higher melting point and higher thermal stability are demanded especially as solid electrolytes for motor vehicles because they work at intermediate temperatures (373–573 K) [27–35]. Such compounds ideally should be obtained as single crystals. Single crystals have a distinct advantage in that their crystal structures can be clearly solved at an atomic level. Accurate elucidation of a material's structure enables us to construct a rational synthetic methodology. Knowing the precise structural design of molecular constituents has allowed for high performance in crystalline hybrid materials [1–3,8,9].

Here recent progress in inorganic–organic hybrid surfactant crystals is briefly overviewed. Organic constituents with long alkyl chain (number of C atoms $\geqslant 8$) are referred to as "surfactants" herein. Hybrid surfactant single crystals are classified into some categories, and their structures and characteristics as functional materials are reviewed.

2. Hybrid Surfactant Single Crystals Constructed by Inorganic Ions

Hybrid surfactant single crystals containing inorganic ions are intrinsically ionic compounds. These crystals are at first classified into two categories: (i) crystals with discrete inorganic metal cations of M^{n+}; and (ii) crystals comprising discrete inorganic anions such as $[MX_4]^{n-}$, $[M_2X_6]^{n-}$, or $[M_4X_{10}]^{n-}$ (X = O, S, Cl, I, *etc.*), including POM cluster anions.

2.1. Hybrid Surfactant Single Crystals with Discrete Inorganic Cations

Hybrid surfactant single crystals containing discrete M^{n+} metal cations are usually metal-coordinated compounds, in which M^{n+} is coordinated by organic surfactant ligands. Of such compounds, the most famous examples are probably chlorophyll molecules involved in photosynthesis in plants (Figure 2) [36,37]. The amphiphilic moiety of chlorophyll enables appropriate arrangements of its magnesium-containing hydroporphyrin moieties, which effectively absorb light as photo antennas. These coordination complexes composed of surfactant ligands [38–65] enable us to control the assembling manner of M^{n+} components in the solid state, owing to the long alkyl chains ("fastener effect") [66]. Moreover, the coordination environments of metal cations can be accurately and flexibly controlled by changing the surfactant ligand structure. This leads to precise design of properties derived from electronic states of the coordinated metal ion. In addition, the surfactant moiety can add liquid crystallinity to metal coordination compounds.

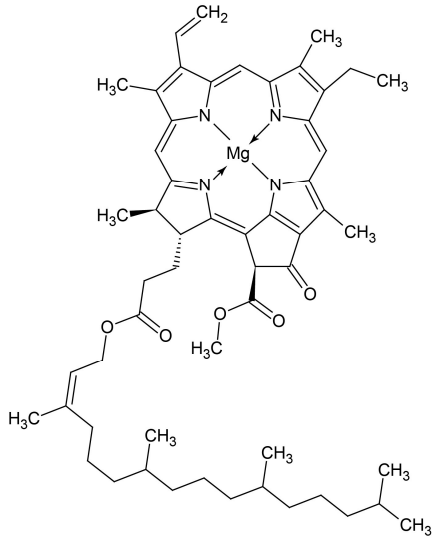

Figure 2. Structure of chlorophyll a_1.

Selected ligands employed in hybrid surfactant single crystals are shown in Figure 3. The structures of the coordinating part are well established in coordination chemistry: monodentate ligands (pyridine [38], 4,4′-bipyridyl [39], imidazole [40–43], *N*-heterocyclic carbene [44–47], phosphine [48]), bidentate ligands (ethylenediamine [49,50], carboxylato [51,52], sulfonato [53], 2,2′-bipyridine [54], 1,10-phenanthroline [55,56], thiolato (μ_2 bridge) [57]), tridentate ligands (terpyridine [58–60], 1,4,7-triazacyclononane [61]), and tetradentate ligands (Schiff base [62–64], 1,3,5,8,12-pentaazacyclotetradecane [65]). Nitrogen atom-containing ligands have often been used, presumably due to the stability and versatility of coordination bonds. Ligands with a coordination number higher than 2 are effective due to the chelate or macrocyclic effect.

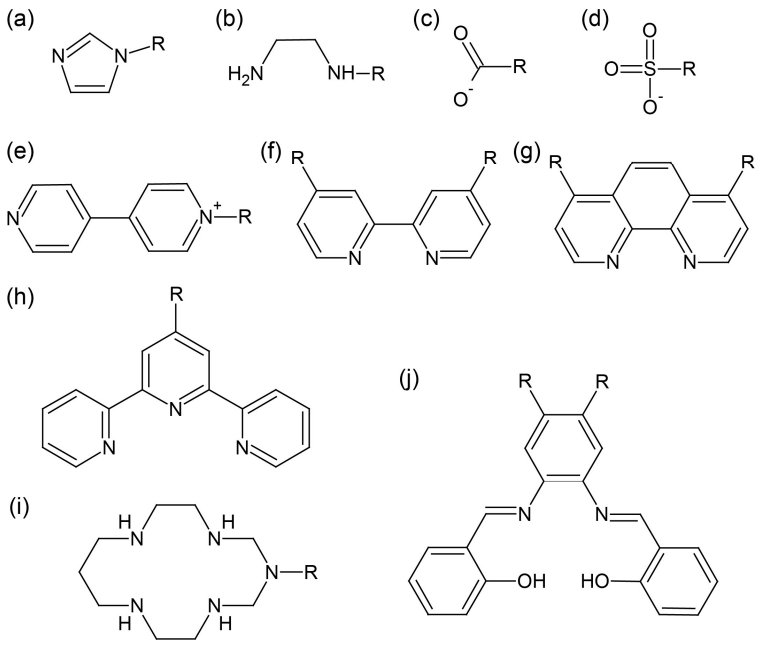

Figure 3. Selected ligands employed in the hybrid surfactant single crystals composed from discrete metal cations: (**a**) imidazole; (**b**) ethylenediamine; (**c**) carboxylato; (**d**) sulfonato; (**e**) 4,4′-bipyridyl; (**f**) 2,2′-bipyridine; (**g**) 1,10-phenanthroline; (**h**) terpyridine; (**i**) 1,3,5,8,12-pentaazacyclotetradecane; (**j**) Schiff base. R in the scheme represents amphiphilic moiety.

Some of their coordination and packing modes are schematically extracted (Figure 4). The coordination mode depends on the number of surfactant ligands to coordinate to the metal cation, and on the number of amphiphilic chains of each ligand. Here, the coordination mode does not mean accurate coordination geometry. There are six typical coordination and packing modes: asymmetric coordination of one single-chained ligand (Figure 4a) [38,39,55,61,65], symmetric coordination of two single-chained ligands lying on the opposite sides of the metal cation (Figure 4b) [41–43,49,51,53,55,59,60], symmetric coordination of one double-chained ligand with two chains at the opposite sides of the metal cation (Figure 4c) [45,47,54,55,62], asymmetric coordination of two single-chained ligands lying on the same side of the metal cation (Figure 4d) [44,46,48,56], asymmetric coordination of one double-chained ligand with narrow space between the chains (Figure 4e) [50,54,63], and asymmetric coordination of one double-chained ligand with wide space between the chains (Figure 4f) [41]. However, the essential feature is the formation of a layered structure that consists of M^{n+} inorganic layers and surfactant organic layers. The long amphiphilic chains are densely packed with or without interdigitation, which depends on the chain length and structure of coordinating moiety. Some ligands possess asymmetric coordination mode (Figure 4a,d–f); however, they usually form symmetric packing in the single crystals. Although it is difficult to strictly categorize these coordination and packing modes due to the variety of the ligand structures, monodentate ligands coordinate in both a symmetric and asymmetric manner (Figure 4a,b). On the other hand, bidentate and tridentate ligands seem to prefer symmetric coordination modes (Figure 4b,c)

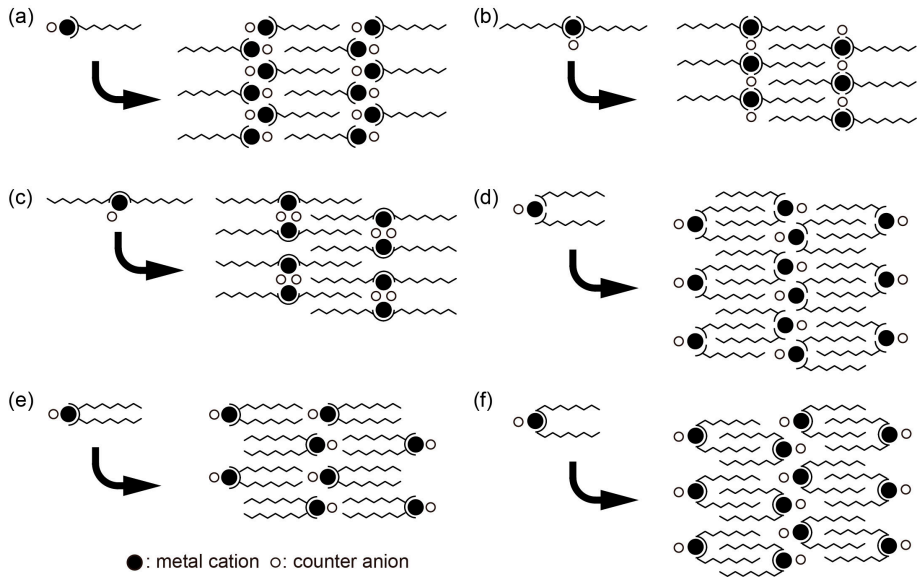

Figure 4. Extracted coordination and packing modes observed in hybrid surfactant single crystals composed from discrete metal cations and surfactant ligands: (**a**) asymmetric coordination of one single-chained ligand; (**b**) symmetric coordination of two single-chained ligands; (**c**) symmetric coordination of one double-chained ligand; (**d**) asymmetric coordination of two single-chained ligands; (**e**) asymmetric coordination of one double-chained ligand with narrow space between the chains; (**f**) asymmetric coordination of one double-chained ligand with wide space between the chains. Here "symmetric" means that amphiphilic chains lie in the opposite sides of metal cation, and "asymmetric" means that amphiphilic chains lie on the same side of the metal cation.

These hybrid surfactant crystals containing coordinated metal M^{n+} cations exhibit spin crossover [56,58–60] and valence tautomerism [38] induced by changes in the coordination environment. Thermal motion in the long amphiphilic chains plausibly affects the electronic spin state of metal cations. These crystals intrinsically can exhibit the phase transition to the liquid crystalline state with an increase in the temperature as metallomesogens [67], and their mesomorphic property

has been investigated [41–46,51,68,69]. Ionic conductivity [70,71], photoluminescence [39,54,62,63], catalytic activity [47,48], thin-film formation ability [39,69], and behavior as preparative precursor for metal nanoparticles [43,57] have been explored recently.

2.2. Hybrid Surfactant Single Crystals with Discrete Inorganic Anions

Hybrid surfactant single crystals containing discrete inorganic anions are ionic salts of amphiphilic surfactant cations and non-amphiphilic inorganic anions [72–90]. The inorganic anions are metal halides, chalcogenides, and oxides, which vary from monomeric anions to highly polymeric anions (Figure 5). Metal oxide cluster-surfactant hybrid crystals are mentioned as polyoxometalate (POM) hybrid crystals in the next section. The examples of monomeric anion are $[ZnCl_4]^{2-}$ [72–74], $[PdCl_4]^{2-}$ [76], $[Co(CO)_4]^{-}$ [79]. Representative polymeric anions are $[Sn_2S_6]^{4-}$ [81], $[Ge_4S_{10}]^{4-}$ [82], $[Ge_4Se_{10}]^{4-}$ [83,84], $[Re_6Se_8(CN)_6]^{4-}$ [85], and infinite planar anion of $[PbI_4]^{2-}$ [87–90]. The minus charge of the inorganic anion is compensated for by the organic surfactant cation (Figure 6). These hybrid crystals composed of discrete inorganic anions are less popular in number and variety than the hybrid crystals consisting of discrete metal cations coordinated by amphiphilic ligands, probably because a more specific combination of inorganic anion and surfactant cation is necessary. The formation of single crystals tends to require size matching between the inorganic anions and hydrophilic heads of surfactant cations, resulting in a specific combination of inorganic and surfactant constituents. Alkylammonium (Figure 6c) [72,80,81,84,86,88] and alkyldiammonium (Figure 6d) [73,89,90] often give single crystals, being different from the case of hybrid surfactant single crystals of coordinated compounds. The primary ammonium cations can form hydrogen bonds between inorganic anions by using N–H bonds to stabilize the crystal structures [87]. However, these ammonium cations are not effective ligands to M^{n+} cations, since the stabilization by the chelate effect cannot be expected.

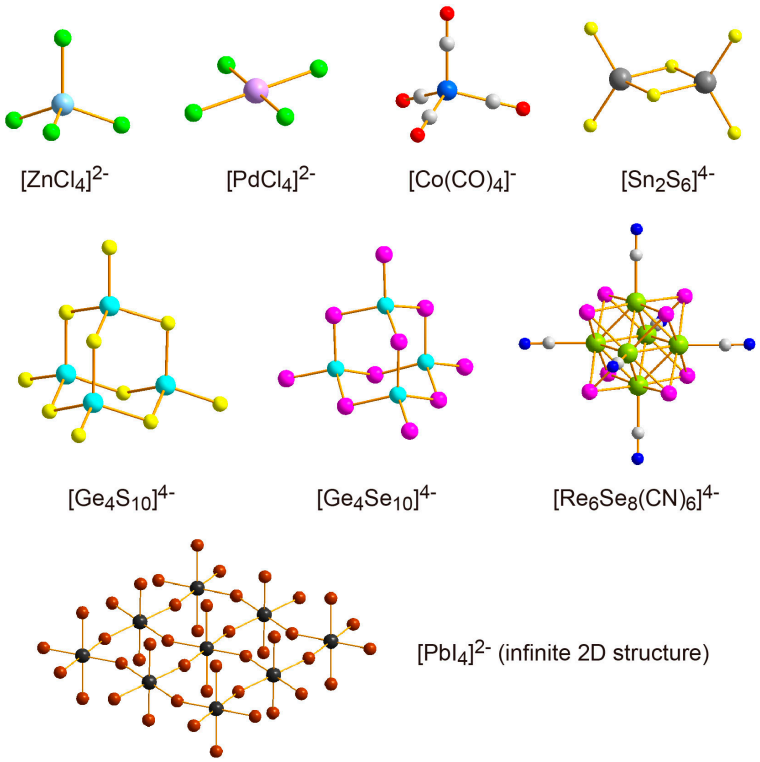

Figure 5. Several discrete inorganic anions employed to construct hybrid surfactant single crystals with cationic surfactants. Oxide cluster anions are represented separately in Figure 7.

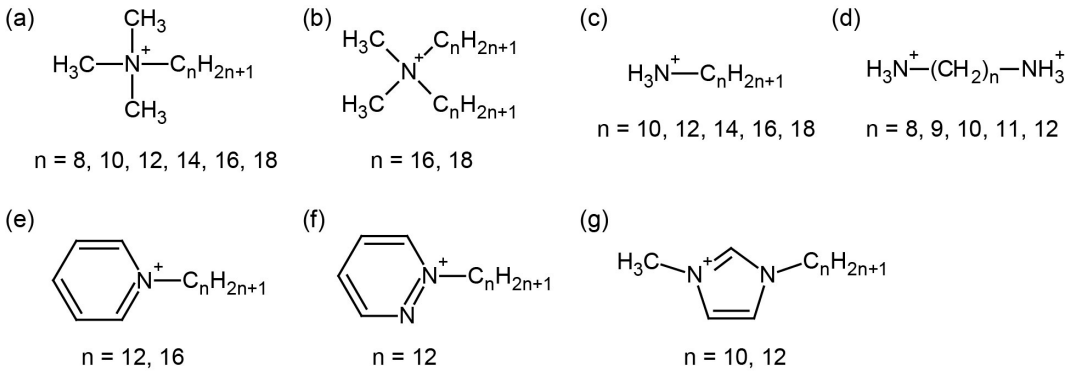

Figure 6. Several cationic surfactants employed to construct hybrid surfactant single crystals with discrete inorganic anions: (**a**) alkyltrimethylammonium; (**b**) dialkyldimethylammonium; (**c**) alkylammonium; (**d**) alkyldiammonium; (**e**) alkylpyridinium; (**f**) alkylpyridazinium; (**g**) 1-alkyl-3-methylimidazolium.

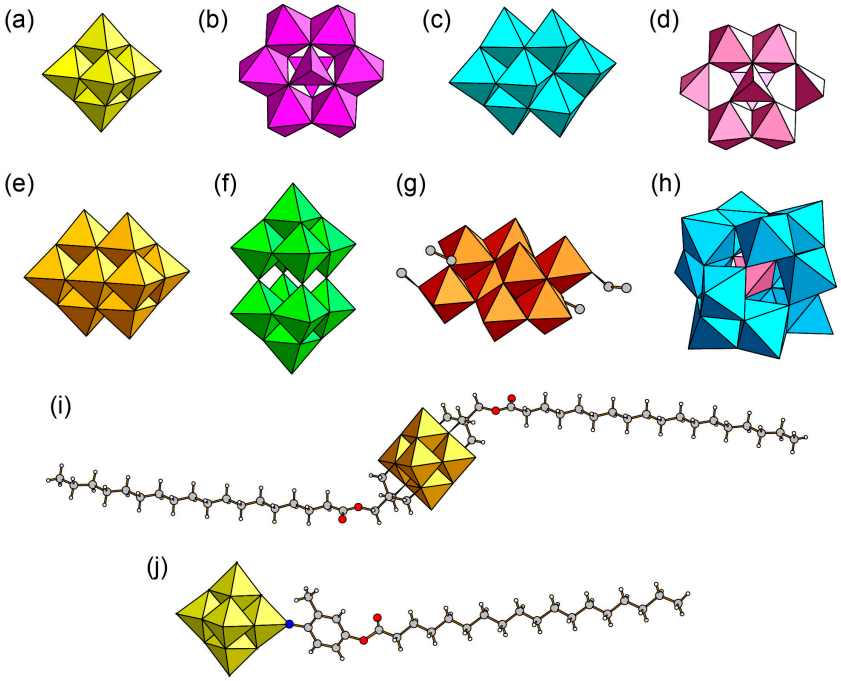

Figure 7. POMs employed for the construction of hybrid surfactant single crystals: (**a**) $[Mo_6O_{19}]^{2-}$ (Mo_6); (**b**) α-$[Mo_8O_{26}]^{4-}$ (α-Mo_8); (**c**) β-$[Mo_8O_{26}]^{4-}$ (β-Mo_8); (**d**) δ-$[Mo_8O_{26}]^{4-}$ (δ-Mo_8); (**e**) $[V_{10}O_{28}]^{6-}$ (V_{10}); (**f**) $[W_{10}O_{32}]^{4-}$ (W_{10}); (**g**) $[\gamma\text{-}Mo_8O_{24}(OC_2H_5)_4]^{4-}$ (γ-Mo_8); (**h**) $[SiMo_{12}O_{40}]^{4-}$ ($SiMo_{12}$); (**i**) $[V_6O_{13}\{(OCH_2)_3CCH_2OOC(CH_2)_{16}CH_3\}_2]^{2-}$; (**j**) $[Mo_6O_{18}(N\text{-}C_6H_3\text{-}2\text{-}(CH_3)\text{-}4\text{-}OCOC_{17}H_{35})]^{2-}$.

The hybrid surfactant crystals containing monomeric inorganic anions typically form layered packing, as shown in Figure 8a. The packing manner comprises alternate stacking of inorganic monolayers and organic surfactant layers. The single-headed surfactant forms a bilayer arrangement to realize a dense packing of long alkyl chains (Figure 8a, left), while the double-headed surfactant forms monolayer structures (Figure 8a, right). When a single-headed and single-chained surfactant is employed, the inorganic layers sometimes form a bilayer structure, probably due to the small size of monomeric ions (Figure 8b) [74,75,79,80]. To compensate for the negative charge of the inorganic anion, the charged hydrophilic heads of the surfactant come close to the anion. The small monomeric anions are necessary to form a bilayer arrangement to increase the number of surfactant cations associated with the monomeric anions.

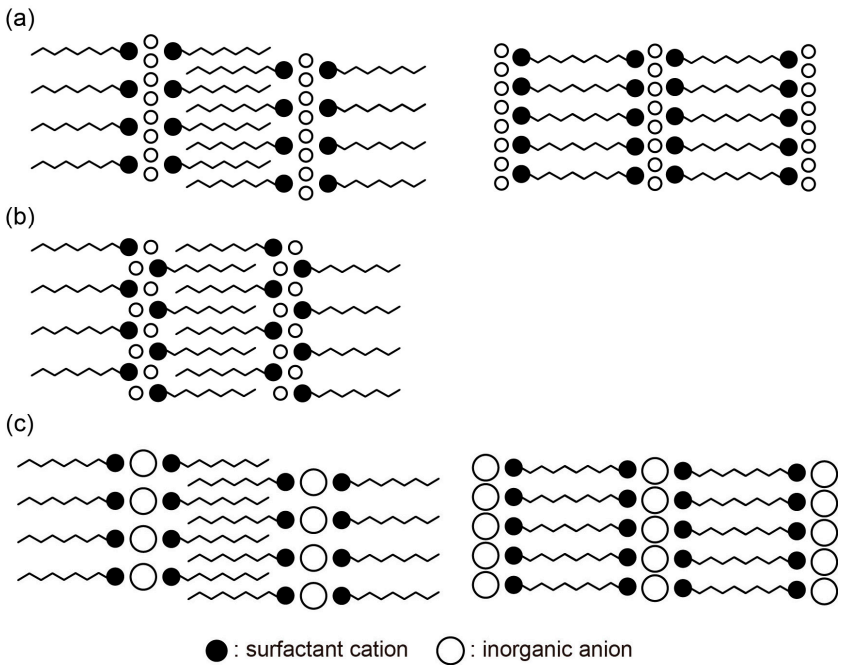

Figure 8. Packing manners observed in the hybrid surfactant single crystals comprised of discrete inorganic anions: (**a**) Monomeric anions hybridized with single-headed surfactant (left) and double-headed surfactant (right); (**b**) monomeric anions to form bilayer arrangement hybridized with single-headed and single-chained surfactant; (**c**) polymeric anions hybridized with single-headed surfactant (left) and double-headed surfactant (right). The inorganic layers depicted by open circles are sometimes polymerized to form infinite two-dimensional layers (see text).

The polymeric anions realize more integrated metal ions confined in the two-dimensional inorganic layer, and are expected to emerge specific electronic properties [10–14,16]. The metal halides tend to form a perovskite-type infinite two-dimensional layered structure [13], which consists of a polymeric metal halide layer such as $[PbI_4]^{2-}$ (Figure 5) [87–90]. On the other hand, metal chalcogenides form molecular cluster anions ($[Sn_2S_6]^{4-}$, $[Ge_4S_{10}]^{4-}$, $[Ge_4Se_{10}]^{4-}$, $[Re_6Se_8(CN)_6]^{4-}$, Figure 5), and are hybridized to form layered single crystals [81–85]. Such molecular cluster-surfactant hybrid single crystals are much more unconventional materials.

The packing feature in the hybrid surfactant single crystals comprised of polymeric inorganic anions is depicted in Figure 8c. The inorganic layers are composed from the monolayer of large molecular cluster anions or an infinite two-dimensional anionic layer. These inorganic monolayers are sandwiched by bilayers of the single-headed surfactant (Figure 8c, left) or monolayers of the double-headed surfactant (Figure 8c, right). Due to the large size of polymeric anions, charged surfactant hydrophilic heads of the surfactant cation can easily access anions, resulting in the monolayer arrangement of the inorganic anions.

Metal halide infinite layers and chalcogenide molecular clusters comprise heavier and more polarizable atoms (S, Cl, Se, Br, and I), and exhibit characteristic electronic property owing to their polymeric structures such as semiconductivity [13,16,82–85,91–94] or photoluminescence [13,16,85,90]. Surfactant hybrid crystals composed from these metal halide and chalcogenide polymeric anions can be applicable to dye-sensitized solar cells [95,96] and electronic devices [97].

3. Hybrid Surfactant Single Crystals Constructed by Polyoxometalates

Polyoxometalates (POMs) are a vast class of molecular oxide cluster anions, the main constituents of which are early transition metals [18]. POMs have a wide variety of physicochemical properties [8,9,18–26], and are promising candidates as inorganic components to construct hybrid

surfactant single crystals. POMs have been hybridized with cationic surfactants to build up inorganic–organic hybrid materials [98–106]. POM-surfactant hybrids can allow fine tuning of the structure and function by changing the combination of POM anion and surfactant cation. Several properties have been investigated as amphiphilic [98–100], magnetic [101], catalytic [102], electrochemical [103], and photoluminescent [103–106] materials.

The layered POM-surfactant hybrids with two-dimensional anisotropy have been assembled as liquid crystals [105], thin films [101,103,106], and mesostructured solids [100,102,107–112]. However, most of them are materials with atomically ill-ordered structure. On the other hand, POM-surfactant single crystals having rigid structures are much rarer hybrids. This is probably because the POM-surfactant hybrids have a larger surfactant cation, which results in lower solubility to crystallize from common solvents. In addition, their anisotropic layered structures often lead to fine needle or thin plate crystals, challenging to analyze by single crystal X-ray structure analysis.

POM-surfactant hybrid layered crystals have been known since 1997 [113], and began to be successfully obtained as single crystals in this decade [113–140]. The layered structure of POM-surfactant crystals comprises alternate stacking of POM monolayers and surfactant bilayers, as shown in Figure 8c. A few crystals possess the bilayer packing manner of POM anions [119,121]. The inorganic POM layer can be considered as an atomically regular two-dimensional POM array, and the molecular arrangement of POM anion is controllable by changing the structures of surfactant hydrophilic head. In addition, the layered distance depends on the structures of the constituent POM and surfactant.

3.1. Hybrid Single Crystals Composed from Polyoxometalates and Surfactant Cations

A major class of POM-surfactant single crystals consists of cationic surfactants (Figure 6) and conventional POM anions [113–136]. Although both POM anions and surfactant cations are typical species, the combination is quite rare. The synthetic methods are based on a simple cation-exchange reaction, and the products are precipitated from a POM-containing mother solution. The methods using precursor species are also applicable [117,122]. This type of POM-surfactant crystals has been obtained by employing POM anions as shown in Figure 7, where dichromate anion ($[Cr_2O_7]^{2-}$) is not shown. Both isopoly- and heteropolyoxometalate anions can form hybrid single crystals with cationic surfactants. Isopolyoxometalates are hexamolybdate ($[Mo_6O_{19}]^{2-}$ (Mo_6), Figure 7a) [117–119], octamolybate isomers (α-, β-, δ-$[Mo_8O_{26}]^{4-}$ (Mo_8), Figure 7b–d) [116,119–125,133–136], decavanadate ($[V_{10}O_{28}]^{6-}$ (V_{10}), Figure 7e) [113,126], decatungstate ($[W_{10}O_{32}]^{4-}$ (W_{10}), Figure 7f) [127,128], and polyoxomolybdate modified by small alkoxo ligands ($[Mo_4O_{10}(OCH_3)_6]^{2-}$ (Mo_4) [129], [γ-$Mo_8O_{24}(OC_2H_5)_4]^{4-}$ (γ-Mo_8), Figure 7g [124]). The presence of isomer molecules in the Mo_8 anion is crucial for controlling the layered structure and chemical composition in the POM-surfactant hybrid crystals, as mentioned below. A molybdenum nanocluster with higher nuclearity ($[Mo_{36}O_{112}(H_2O)_{16}]^{8-}$) can form hybrid single crystals [132]. Heteropolyoxometalate hybrid crystals contain oxidized and reduced forms of silicomolybdate ($[SiMo_{12}O_{40}]^{4-}$ ($SiMo_{12}$), Figure 7h) [130,131].

Two types of surfactant cations can be selected for the synthesis: (i) a surfactant with a single hydrophilic head; or (ii) a surfactant with two hydrophilic heads. Single-headed surfactants contain alkyltrimethylammonium ($[C_nH_{2n+1}N(CH_3)_3]^+$ (C_nNC_3), Figure 6a) [113,115,116,119,125,126,130,131], dialkyldimethylammonium ($[(C_nH_{2n+1})_2N(CH_3)_2]^+$ ($(C_n)_2NC_2$), Figure 6b) [114,117], or alkylammonium derived from primary amine ($[C_nH_{2n+1}NH_3]^+$ (C_nNH_3), Figure 6c) [123]. In addition, heterocyclic surfactants such as pyridinium ($[C_5H_5N(C_nH_{2n+1})]^+$ ($C_n$py), Figure 6e) [118,120–122,127–129], pyridazinium ($[C_4H_4N_2(C_nH_{2n+1})]^+$ ($C_n$pda), Figure 6f) [128], and methylimidazolium ($[(C_nH_{2n+1})C_3H_3N_2(CH_3)]^+$ ($C_n$mim), Figure 6g) [123,124] are employed. Double-headed surfactants employed are alkyldiammonium derived from diamine ($[H_3N(CH_2)_nNH_3]^{2+}$ ($H_3NC_nNH_3$), Figure 6d) [132,133] or synthetic bolaamphiphiles having two charged heterocyclic moieties [134–136].

These POM-surfactant crystals can flexibly select both inorganic and organic components, leading to promising functional inorganic–organic hybrids.

The layered structures are controllable by changing the length of surfactant alkyl chain [125]. The case of hybrid crystals comprising Mo_8 and C_nNC_3 (n = 8, 10, 12, 14, 16, 18) is shown in Figure 9. Interestingly, there are two types of homologue structure, which change owing to the surfactant length (Figure 9a,b). Shorter surfactants prefer β-Mo_8 isomer, while longer ones prefer δ-Mo_8 isomer, conceivably due to the effect of van der Waals interactions between the surfactant alkyl chains. Such a structural change in isomer molecules induced by the surfactant chain length is rather unique. The layered distances of the C_nNC_3-δ-Mo_8 crystals (n = 12, 14, 16, 18) depend linearly on the surfactant length (Figure 9c).

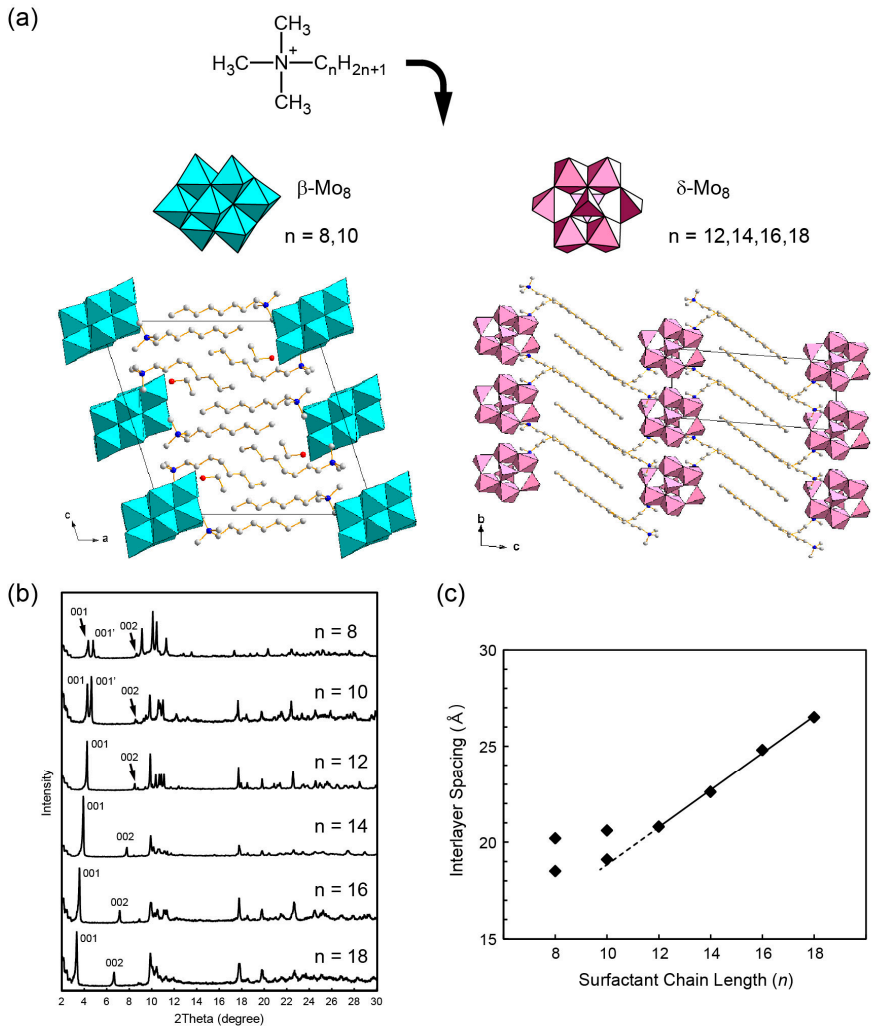

Figure 9. (**a**) Crystal structures of C_nNC_3–Mo_8 hybrid crystals; (**b**) powder X-ray diffraction patterns of as-prepared C_nNC_3-Mo_8; (**c**) variation of the interlayer spacing of as-prepared C_nNC_3–Mo_8 with n [125]. Reproduced with permission from Ito, T. *et al.*, *J. Mol. Struct.*; published by Elsevier, 2016.

Molecular arrangements of POMs are also controllable by changing the structure of surfactant hydrophilic heads, because POMs strongly interact with hydrophilic moieties of employed surfactants. Heterocyclic moieties of $C_n$py, $C_n$pda, and $C_n$mim surfactants fully penetrate into POM inorganic layers to isolate each POM anion in many cases [118,120,123,127,128]. The difference in the molecular structures of the heterocyclic moiety causes different arrangements of W_{10} anions [128]. On the other hand, less bulky heads of C_nNH_3, C_nNC_3, and $(C_n)_2NC_2$ tend to keep POM anions close,

leading to a more densely-packed arrangement of POM anions. In the case of β-Mo_8 hybrid crystals, $C_{12}NH_3$ cations do not completely isolate the β-Mo_8 anions to result in the close arrangement in the β-Mo_8 layers (Figure 10a), while more bulky hydrophilic heads of C_{12}mim penetrate into the β-Mo_8 layers, resulting in the complete isolation of each β-Mo_8 anion (Figure 10b) [123]. C_nNC_3-V_{10} (n = 10, 12) [113,126] and $(C_{18})_2NC_2$-Mo_6 [117] also have rather dense packing of POM anions. Such controllability in molecular arrangement and distance would affect the emergence of conductive or magnetic property.

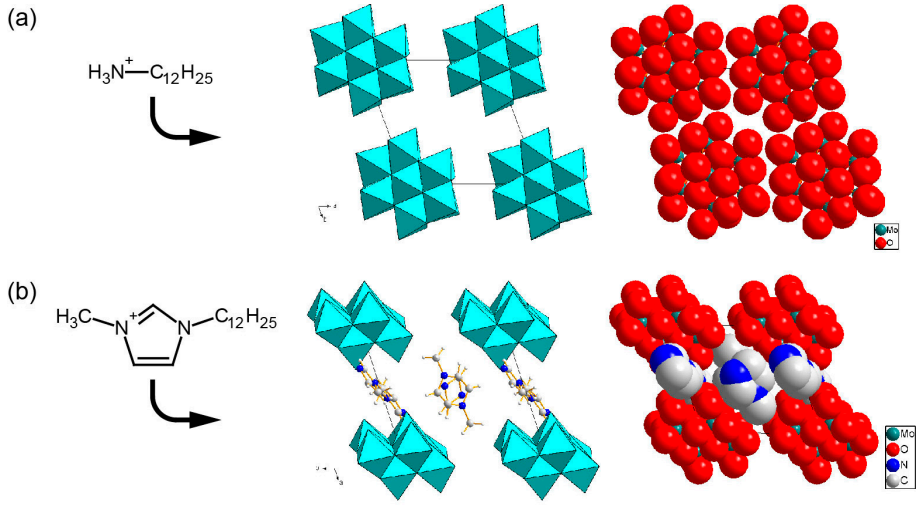

Figure 10. Molecular arrangements of the inorganic layers in β-Mo_8 hybrid crystals. The same arrangements are depicted in polyhedral (left) and space-filling (right) representations. (**a**) $C_{12}NH_3$-β-Mo_8; (**b**) C_{12}mim-β-Mo_8 [123]. Reproduced with permission from Ito, T. *et al.*, *Chem. Lett.*; published by The Chemical Society of Japan, 2013.

One option for the functionalized POM-surfactant crystals is to introduce other countercations such as proton or sodium into the crystal structures as well as surfactant cations. The crystals containing β-type Mo_8 anions tend to crystallize with small countercations such as proton or sodium [120–122,124], and are promising candidates for the solid electrolyte for fuel-cell or sodium-ion batteries. The surfactant hybrid crystals containing small countercations are limited to the crystals consisting of β-Mo_8, γ-Mo_8, and V_{10} to date. Figure 11a shows the crystal structure of a proton-containing Mo_8 hybrid crystal, which has been synthesized by gradual oxidation of reduced polyoxomolybdate-surfactant hybrids [122]. In this crystal, a Mo_8 anion with a charge of 4− is associated with two C_{16}py surfactant cations. The remaining minus charge is compensated for by two protons to form a diprotonated β-Mo_8 anion, which has been confirmed by bond-valence-sum (BVS) calculations. Interestingly, the inorganic layers are two-dimensional anionic layers composed of Mo_8 anions and ethanol molecules of crystallization (Figure 11a, right). The pyridine rings of the surfactants are not penetrated into the inorganic layer, implying the emergence of a surfactant-cation exchange. Another proton-containing hybrid crystal can be obtained by using V_{10} and $C_{10}NC_3$, and the V_{10} anions are diprotonated species (Figure 11b). The presence of protons has been clearly identified by the X-ray structure analysis [126]. In the $C_{10}NC_3$-V_{10} crystal, the diprotonated V_{10} anions are hydrogen-bonded to form a one-dimensional infinite chain structure (Figure 11b, right). The hydrogen-bonded V_{10} chains are closely located (the distance between each chain: 3.25 Å), and not completely isolated by the $C_{10}NC_3$ cations as mentioned above. The inorganic layer composed of hydrogen-bonded V_{10} infinite chains is considered a "pseudo two-dimensional" layer of diprotonated V_{10} anions. The close distance between protonated V_{10} infinite chains would possibly contribute to the emergence of proton conductivity, as described below.

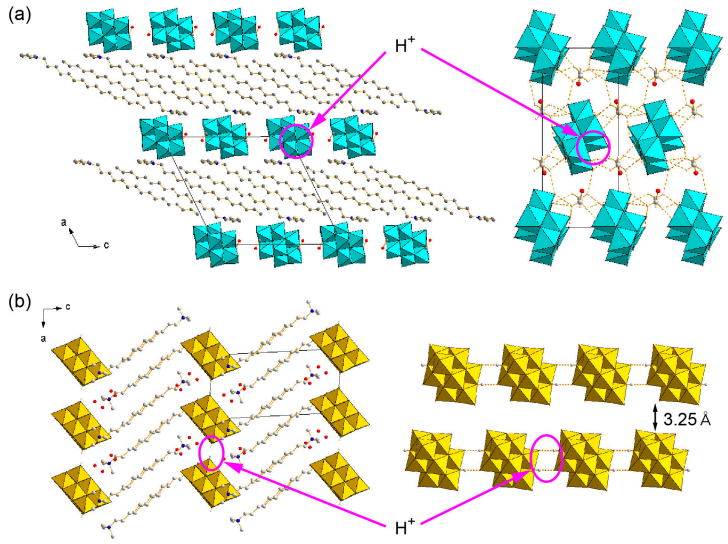

Figure 11. Proton-containing POM-surfactant crystals (left: crystal packing, right: molecular arrangement in the inorganic layer). (**a**) C_{16}py-β-Mo_8 [122]; (**b**) $C_{10}NC_3$-V_{10} [126]. Reproduced with permission from Mikurube, K. *et al.*, *J. Chem.*; published by Hindawi Publishing Corporation, 2013 and from Ito, T. *et al.*, *Bull. Chem. Soc. Jpn.*; published by The Chemical Society of Japan, 2012.

Sodium ion–containing hybrid crystals of Mo_8 can be synthesized in the presence of a sodium ion by using $C_n$py or $C_n$mim (Figure 12) [120,121,124]. In cases where a C_{16}py cation is employed, one β-Mo_8 anion having a charge of 4− is associated with three C_{16}py surfactant cations and one sodium cation [120,121]. A one-dimensional chain structure composed from Mo_8 and a sodium cation is formed (Figure 12b, upper). Different types of sodium ion–containing hybrid crystals have been obtained by using ionic liquid $C_n$mim (n = 10, 12) surfactant cations (Figure 12a) [124]. Notably in these cases, two sodium ions as well as two $C_n$mim cations are contained per one β- or γ-Mo_8 having a charge of 4−, different from the C_{16}py-β-Mo_8 hybrid crystals. In the $C_n$mim-Mo_8 hybrid crystals, two sodium cations connect Mo_8 anions to form infinite one-dimensional chain structures (Figure 12b, bottom).

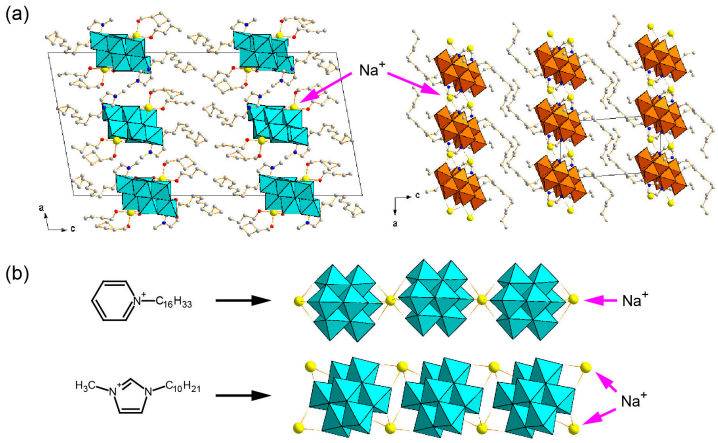

Figure 12. Sodium ion-containing POM-surfactant crystals. (**a**) C_{10}mim-β-Mo_8 (left) and C_{12}mim-γ-Mo_8 (right); (**b**) difference in the arrangements of β-Mo_8 anion and sodium cation depending on the surfactant cation [120,121,124]. Reproduced with permission from Ito, T. *et al.*, *Chem. Lett.*; published by The Chemical Society of Japan, 2010; from Ito, T. *et al.*, *Chem. Lett.*; published by The Chemical Society of Japan, 2011; and from Ito, T. *et al.*, *Crystals;* published by MDPI, 2014.

Conductive property has been investigated for some POM-surfactant hybrid crystals. The measurements were carried out using the alternating current (AC) impedance method for a pelletized sample under an anhydrous atmosphere at intermediate temperature. Electronic conductivities for hybrid crystals of C_{16}py-W_{10} (Figure 13) [127] and C_{16}py-Mo_4 [129] are in the range of 10^{-6} to 10^{-5} S cm^{-1} order. Although these values are much lower than the radical salts of POM containing an organic donor [8,9], POM-surfactant crystals with an appropriate combination of POMs and surfactants would be possible for another class of hybrid solid electrolytes. On the other hand, the proton-containing $C_{10}NC_3$–V_{10} hybrid crystal exhibits anhydrous proton conductivity of 6.5×10^{-5} S cm^{-1} at 373 K [126]. Emergence of anhydrous proton conductivity at intermediate temperatures is demanded for solid electrolyte application for fuel-cell technology [29–33]. Although the proton conductivity of $C_{10}NC_3$–V_{10} is rather unstable and lower than other POM hybrid materials [34,35], the proton-containing POM-surfactant crystals would pave the way for an unprecedented class of proton conductors.

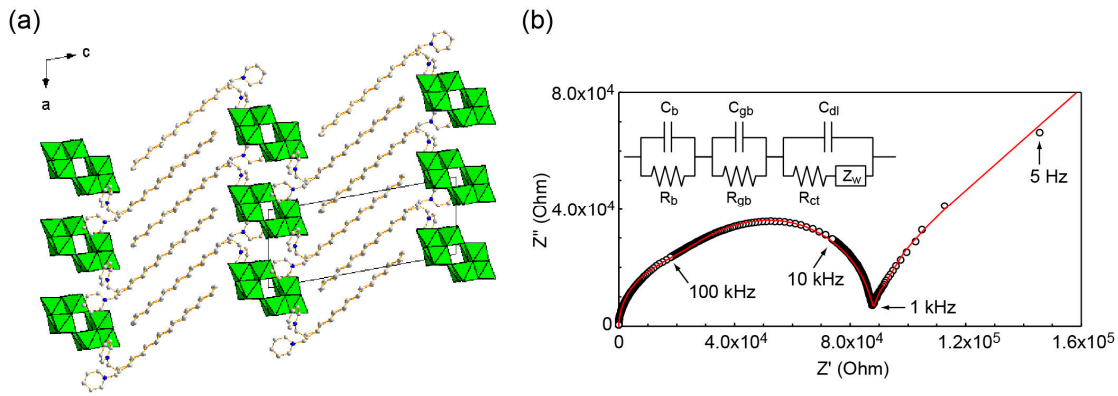

Figure 13. Crystal structure and conductive property of C_{16}py–W_{10} hybrid crystals. (**a**) Crystal packing; (**b**) Nyquist spectrum (open circles) at 423 K and simulated spectrum (**red** line) based on an equivalent electronic circuit [127]. Reproduced with permission from Ito, T. *et al.*, *Crystals;* published by MDPI, 2012.

The redox property, which characterizes POMs as specific functional materials [25,26], has also been investigated. Electrochemical property has been measured in solution state for $C_{16}NC_3$-$SiMo_{12}$ and its reduced hybrids [130,131]. A $(C_{18})_2NC_2$–Mo_6 hybrid crystal containing a double-chained surfactant has been found to form a self-assembled helical structure in dichloromethane/propanol solution [141]. This helical structure exhibits reversible transformation into spherical assemblies with accompanying photoreduction by UV light irradiation, and back to helical assemblies by H_2O_2 oxidation. Catalytic behavior is another characteristic of POM anions [24]. Catalytic oxidation of acetaldehyde with H_2O_2 has been explored for bolaamphiphilic 1,ω-bis(pyridinium)alkane-Mo_8 hybrid crystals (ω = 8–12) [134].

3.2. Hybrid Single Crystals Composed from Polyoxometalate Modified by Amphiphilic Moiety

A recent class of POM-surfactant hybrid crystals is single crystals composed from POMs having amphiphilic moiety [137–140]. In this type of POM-surfactant crystals, amphiphilic POMs are synthesized by grafting a long alkyl chain covalently into pre-modified or lacunary POM anion by condensation reaction such as esterification [22,23]. Several types of POMs with amphiphilic moiety (moieties) have been synthesized [98–100,112,142–149] from Lindqvist-, Anderson-, and Keggin-type anions. However, the amphiphilic POMs analyzed from single crystals have been limited to hexavanadate and hexamolybdate derivatives so far. Anderson-type amphiphilic POMs have been reported to crystallize; however, the crystal structures have not been fully solved due to severe disorder of the amphiphilic moieties [140]. The hexavanadate

derivatives are single-chained $[V_6O_{13}(OCH_2)_3CNH_2(OCH_2)_3CNHCH_2C_6H_4COOC_{16}H_{33}]^{2-}$ [138] and double-chained $[V_6O_{13}\{(OCH_2)_3CCH_2OOC(CH_2)_{16}CH_3\}_2]^{2-}$ (Figure 7i) [137]. The hexamolybdate derivative is single-chained $[Mo_6O_{18}(N\text{-}C_6H_3\text{-}2\text{-}(CH_3)\text{-}4\text{-}OCOC_{17}H_{35})]^{2-}$ (Figure 7j) [139]. In these three cases, amphiphilic POMs having a charge of 2− crystallize with a tetrabutylammonium cation (TBA). The packing manners consist of alternate stacking of an inorganic layer of POM cluster moiety and an organic layer of amphiphilic moiety, being essentially similar to those observed in most POM-surfactant hybrid crystals. Single-chained amphiphilic POMs comprise bilayer arrangements of POMs [138,139], while a double-chained amphiphilic POM has a monolayer arrangement of POM moiety [137]. The difference in the amphiphilicity due to the number of the long alkyl chain may cause the different packing manner of amphiphilic POM layers. As for these crystals, cation exchange to protons from TBA induces characteristic fluorescence [137] and catalysis [138], which demonstrates a wide potential of amphiphilic POMs for functional materials.

4. Summary and Outlook

Hybrid surfactant single crystals containing an inorganic moiety have been evaluated in the search for unprecedented functional materials. Layered crystals composed of inorganic layers and surfactant layers are obtained due to the template effect of a long alkyl chain moiety. These crystalline layered structures create the anisotropic arrangement of the inorganic component, which accounts for the emergence of conductivity [7–9], two-dimensional confinement of magnetic molecules [10], photocatalytic activity [11,12], and controlled luminescence [14,150].

The composition, crystal packing, and molecular arrangement of these hybrid single crystals are controllable by changing the inorganic constituents and surfactant moieties. There are two types of hybrid surfactant single crystals: (i) crystals consisting of a discrete inorganic cation coordinated by ligands having amphiphilic moiety; and (ii) crystals composed from discrete inorganic anion hybridized with surfactant cation. The crystals consisting of a discrete inorganic cation are suitable for controlling the coordination environment of metal cations, resulting in precisely controlled properties such as magnetism [56,58,151,152] or photoluminescence [153–155]. On the other hand, crystals composed from discrete inorganic anions, including infinite two-dimensionally polymerized anions and molecular cluster anions, can confine the metal components in the layered structures, which leads to characteristic electronic properties [13,16] and device applications [95–97,156–158].

Some of the most promising functional inorganic anions are polyoxometalate (POM) cluster anions. POM-surfactant hybrid single crystals, which are comprised of alternate inorganic POM layers and organic surfactant layers, have been synthesized recently. POM-surfactant crystals containing a typical POM anion and a surfactant cation have been obtained via a simple cation-exchange reaction. Changing POM and surfactant molecular structures enables us to control the layered structure including two-dimensional POM arrangement, and to introduce a small countercation such as proton or sodium. Conductivity, redox property, and catalytic behavior have been explored. In addition, amphiphilic POMs have been reported to form single crystals, and to exhibit characteristic properties owing to the POM moiety. This type of POMs possesses a long alkyl chain moiety covalently grafted directly onto a POM skeleton.

There are still several difficulties to overcome for the synthesis, structural prediction, and structure analysis of hybrid surfactant single crystals. The distinct crystal and molecular structures are difficult to analyze, since their crystals are often tiny and anisotropic (thin plates or fine fibers). To obtain suitable single crystals sometimes requires slow crystal growth under mild conditions. Effective options are to adjust the appropriate concentration of the dissolved sample and keep the temperature constant during the crystallization. Synchrotron radiation is a powerful method for measurement. Powder diffraction methods are difficult to apply to solving the structures of hybrid surfactant crystal containing many heavy metals such as POM clusters, because the position of the light atoms (C and N) in the surfactant moiety is difficult to discern due to their weak reflections in the diffraction data. In addition, the emergence of characteristic properties is still developing; more intentional design of

built-up hybrid crystals is needed. However, these difficulties deserve to be tackled in order to explore the synthesis and functionalization of hybrid surfactant single crystals.

Acknowledgments: Shinichi Koguchi is acknowledged for valuable comments. This work was supported in part by a JSPS Grant-in-Aid for Scientific Research (No. 26410245), and a Research and Study Project of the Tokai University Educational System General Research Organization.

Conflicts of Interest: The author declares no conflict of interest.

References

1. Yaghi, O.M.; O'Keeffe, M.; Ockwig, N.W.; Chae, H.K.; Eddaoudi, M.; Kim, J. Reticular synthesis and the design of new materials. *Nature* **2003**, *423*, 705–714. [CrossRef] [PubMed]
2. Kitagawa, S.; Kitaura, R.; Noro, S. Functional porous coordination polymers. *Angew. Chem. Int. Ed.* **2004**, *43*, 2334–2375. [CrossRef] [PubMed]
3. Maurizot, V.; Yoshizawa, M.; Kawano, M.; Fujita, M. Control of molecular interactions by the hollow of coordination cages. *Dalton Trans.* **2006**, 2750–2756. [CrossRef] [PubMed]
4. Ruiz-Hitzky, E.; Aranda, P.; Darder, M.; Ogawa, M. Hybrid and biohybrid silicate based materials: Molecular *vs.* block-assembling bottom–up processes. *Chem. Soc. Rev.* **2011**, *40*, 801–828. [CrossRef] [PubMed]
5. Schubert, U. Cluster-based inorganic-organic hybrid materials. *Chem. Soc. Rev.* **2011**, *40*, 575–582. [CrossRef] [PubMed]
6. Kato, T.; Mizoshita, M.; Kishimoto, K. Functional liquid-crystalline assemblies: Self-organized soft materials. *Angew. Chem. Int. Ed.* **2006**, *45*, 38–68. [CrossRef] [PubMed]
7. Casciola, M. Ionic conductivity in layered materials. In *Comprehensive Supramolecular Chemistry*; Atwood, J.L., Davies, J.E.D., MacNicol, D.D., Vögtle, F., Eds.; Elsevier Science: Oxford, UK, 1996; Volume 7, pp. 355–378.
8. Coronado, E.; Gómez-García, C.J. Polyoxometalate-based molecular materials. *Chem. Rev.* **1998**, *98*, 273–296. [CrossRef] [PubMed]
9. Coronado, E.; Giménez-Saiz, C.; Gómez-García, C.J. Recent advances in polyoxometalate-containing molecular conductors. *Coord. Chem. Rev.* **2005**, *249*, 1776–1796. [CrossRef]
10. Clemente-León, M.; Coronado, E.; Martí-Gastaldo, C.; Romero, F.M. Multifunctionality in hybrid magnetic materials based on bimetallic oxalate complexes. *Chem. Soc. Rev.* **2011**, *40*, 473–497. [CrossRef] [PubMed]
11. Domen, K.; Kondo, J.N.; Hara, M.; Takata, T. Photo- and mechano-catalytic overall water spiliing reaction to form hydrogen and oxygen on heterogeneous catalysts. *Bull. Chem. Soc. Jpn.* **2000**, *73*, 1307–1331. [CrossRef]
12. Kudo, A.; Miseki, Y. Heterogeneous photocatalyst materials for water splitting. *Chem. Soc. Rev.* **2009**, *38*, 253–278. [CrossRef] [PubMed]
13. Mitzi, D.B. Synthesis, structure, and properties of organic-inorganic perovskites and related materials. *Prog. Inorg. Chem.* **1999**, *48*, 1–121.
14. Aliprandi, A.; Mauro, M.; De Cola, L. Controlling and imaging biomimetic self-assembly. *Nat. Chem.* **2016**, *8*, 10–15. [CrossRef] [PubMed]
15. Huo, Q.; Margolese, D.I.; Ciesla, U.; Demuth, D.G.; Feng, P.; Gier, T.E.; Sieger, P.; Firouzi, A.; Chmelka, B.F.; Schüth, F.; *et al*. Organization of organic molecules with inorganic molecular species into nanocomposite biphase arrays. *Chem. Mater.* **1994**, *6*, 1176–1191. [CrossRef]
16. Kanatzidis, M.G. Beyond silica: Nonoxidic mesostructured materials. *Adv. Mater.* **2007**, *19*, 1165–1181. [CrossRef]
17. Yamauchi, Y.; Kuroda, K. Rational design of mesoporous metals and related nanomaterials by a soft-template approach. *Chem. Asian J.* **2008**, *3*, 664–676. [CrossRef] [PubMed]
18. Pope, M.T. *Heteropoly and Isopoly Oxometalates*; Springer: Berlin, Germany, 1983.
19. Cronin, L.; Müller, A. Polyoxometalate cluster science. *Chem. Soc. Rev.* **2012**, *41*, 7325–7648.
20. Long, D.-L.; Burkholder, E.; Cronin, L. Polyoxometalate clusters, nanostructures and materials: From self assembly to designer materials and devices. *Chem. Soc. Rev.* **2007**, *36*, 105–121. [CrossRef] [PubMed]
21. Nyman, M. Polyoxoniobate chemistry in the 21st century. *Dalton Trans.* **2011**, *40*, 8049–8058. [CrossRef] [PubMed]
22. Gouzerh, P.; Proust, A. Main-group element, organic, and organometallic derivatives of polyoxometalates. *Chem. Rev.* **1998**, *98*, 77–111. [CrossRef] [PubMed]

23. Proust, A.; Matt, B.; Villanneau, R.; Guillemot, G.; Gouzerh, P.; Izzet, G. Functionalization and post-functionalization: A step towards polyoxometalate-based materials. *Chem. Soc. Rev.* **2012**, *41*, 7605–7622. [CrossRef] [PubMed]
24. Okuhara, T.; Mizuno, N.; Misono, M. Catalytic chemistry of heteropoly compounds. *Adv. Catal.* **1996**, *41*, 113–252.
25. Yamase, T. Photo- and electrochromism of polyoxometalates and related materials. *Chem. Rev.* **1998**, *98*, 307–325. [CrossRef] [PubMed]
26. Sadakane, M.; Steckhan, E. Electrochemical properties of polyoxometalates as electrocatalysts. *Chem. Rev.* **1998**, *98*, 219–237. [CrossRef] [PubMed]
27. Whittingham, M.S. Lithium batteries and cathode materials. *Chem. Rev.* **2004**, *104*, 4271–4301. [CrossRef] [PubMed]
28. Kamaya, N.; Homma, K.; Yamakawa, Y.; Hirayama, M.; Kanno, R.; Yonemura, M.; Kamiyama, T.; Kato, Y.; Hama, S.; Kawamoto, K.; *et al*. A lithium superionic conductor. *Nat. Mater.* **2011**, *10*, 682–686. [CrossRef] [PubMed]
29. Steele, B.C.H.; Heinzel, A. Materials for fuel-cell technologies. *Nature* **2001**, *414*, 345–352. [CrossRef] [PubMed]
30. Yoon, M.; Suh, K.; Natarajan, S.; Kim, K. Proton conduction in metal-organic frameworks and related modularly built porous solids. *Angew. Chem. Int. Ed.* **2013**, *52*, 2688–2700. [CrossRef] [PubMed]
31. Hurd, J.A.; Vaidhyanathan, R.; Thangadurai, V.; Ratcliffe, C.I.; Moudrakovski, I.L.; Shimizu, G.K.H. Anhydrous proton conduction at 150 °C in a crystalline metal-organic framework. *Nat. Chem.* **2009**, *1*, 705–710. [CrossRef] [PubMed]
32. Bureekaew, S.; Horike, S.; Higuchi, H.; Mizuno, M.; Kawamura, T.; Tanaka, D.; Yanai, N.; Kitagawa, S. One-dimensional imidazole aggregate in aluminium porous coordination polymers with high proton conductivity. *Nat. Mater.* **2009**, *8*, 831–836. [CrossRef] [PubMed]
33. Yamada, T.; Sadakiyo, M.; Kitagawa, H. High proton conductivity of one-dimensional ferrous oxalate dihydrate. *J. Am. Chem. Soc.* **2009**, *131*, 3144–3145. [CrossRef] [PubMed]
34. Honma, I.; Yamada, M. Bio-inspired membranes for advanced polymer electrolyte fuel cells. Anhydrous proton-conducting membrane via molecular self-assembly. *Bull. Chem. Soc. Jpn.* **2007**, *80*, 2110–2123. [CrossRef]
35. Oh, S.-Y.; Yoshida, T.; Kawamura, G.; Muto, H.; Sakai, M.; Matsuda, A. Inorganic-organic composite electrolytes consisting of polybenzimidazole and Cs-substituted heteropoly acids and their application for medium temperature fuel cells. *J. Mater. Chem.* **2010**, *20*, 6359–6366. [CrossRef]
36. Deisenhofer, J.; Epp, O.; Miki, K.; Huber, R.; Michel, H. X-ray structure analysis of a membrane protein complex. Electron density map at 3 Å resolution and a model of the chromophores of the photosynthetic reaction center from Rhodopseudomonas viridis. *J. Mol. Biol.* **1984**, *180*, 385–398. [CrossRef]
37. Deisenhofer, J.; Epp, O.; Miki, K.; Huber, R.; Michel, H. Structure of the protein subunits in the photosynthetic reaction centre of Rhodopseudomonas viridis at 3Å resolution. *Nature* **1985**, *318*, 618–624. [CrossRef] [PubMed]
38. Kiriya, D.; Chang, H.C.; Kitagawa, S. Molecule-based valence tautomeric bistability synchronized with a macroscopic crystal-melt phase transition. *J. Am. Chem. Soc.* **2008**, *130*, 5515–5522. [CrossRef] [PubMed]
39. Boubekeur-Lecaque, L.; Coe, B.J.; Harris, J.A.; Helliwell, M.; Asselberghs, I.; Clays, K.; Foerier, S.; Verbiest, T. Incorporation of amphiphilic ruthenium(II) ammine complexes into Langmuir-Blodgett thin films with switchable quadratic nonlinear optical behavior. *Inorg. Chem.* **2011**, *50*, 12886–12899. [CrossRef] [PubMed]
40. Lin, I.J.B.; Vasam, C.S. Metal-containing ionic liquids and ionic liquid crystals based on imidazolium moiety. *J. Organomet. Chem.* **2005**, *690*, 3498–3512. [CrossRef]
41. Lee, C.K.; Ling, M.J.; Lin, I.J.B. Organic-inorganic hybrids of imidazole complexes of palladium(II), copper(II) and zinc(II). Crystals and liquid crystals. *Dalton Trans.* **2003**, 4731–4737. [CrossRef]
42. Lee, C.K.; Hsu, K.-M.; Tsai, C.-H.; Lai, C.K.; Lin, I.J.B. Liquid crystals of silver complexes derived from simple 1-alkylimidazoles. *Dalton Trans.* **2004**, 1120–1126. [CrossRef] [PubMed]
43. Hsu, S.J.; Hsu, K.M.; Leong, M.K.; Lin, I.J.B. Au(I)-benzimidazole/imidazole complexes. Liquid crystals and nanomaterials. *Dalton Trans.* **2008**, 1924–1931. [CrossRef] [PubMed]
44. Lee, K.M.; Lee, C.K.; Lin, I.J.B. A facile synthesis of unusual liquid-crystalline gold(I) dicarbene compounds. *Angew. Chem. Int. Ed.* **1997**, *36*, 1850–1852. [CrossRef]

45. Lee, C.K.; Chen, J.C.C.; Lee, K.M.; Liu, C.W.; Lin, I.J.B. Thermally stable mesomorphic palladium(II)-carbene complexes. *Chem. Mater.* **1999**, *11*, 1237–1242. [CrossRef]
46. Hsu, T.H.T.; Naidu, J.J.; Yang, B.-J.; Jang, M.-Y.; Lin, I.J.B. Self-assembly of silver(I) and gold(I) *N*-heterocyclic carbene complexes in solid state, mesophase, and solution. *Inorg. Chem.* **2012**, *51*, 98–108. [CrossRef] [PubMed]
47. Ohta, H.; Fujihara, T.; Tsuji, Y. *N*-Heterocyclic carbene ligands bearing hydrophilic and/or hydrophobic chains: Rh(I) and Pd(II) complexes and their catalytic activity. *Dalton Trans.* **2008**, 379–385. [CrossRef]
48. Polas, A.; Wilton-Ely, J.D.E.T.; Slawin, A.M.Z.; Foster, D.F.; Steynberg, P.J.; Green, M.J.; Cole-Hamilton, D.J. Limonene-derived phosphines in the cobalt-catalysed hydroformylation of alkenes. *Dalton Trans.* **2003**, 4669–4677. [CrossRef]
49. Iida, M.; Tanase, T.; Asaoka, N.; Nakanishi, A. A molecular structure of bis(*N*-octylethylenediamine)zinc(II) nitrate crystal and the aggregations in wet chloroform and benzene solutions. *Chem. Lett.* **1998**, *27*, 1275–1276. [CrossRef]
50. Arulsamy, N.; Bohle, D.S.; Goodson, P.A.; Jaeger, D.A.; Reddy, V.B. Synthesis, structure, and spectrochemistry of double-chain surfactant Co(III) complexes. *Inorg. Chem.* **2001**, *40*, 836–842. [CrossRef]
51. Elliott, J.M.; Chipperfield, J.R.; Clark, S.; Teat, S.J.; Sinn, E. Criteria for liquid crystal formation in 5-alkoxy-, 5-alkylamino-, and 5-alkanoyl-tropolone complexes of transition metals (Cu^{II}, Zn^{II}, Ni^{II}, Co^{II}, $UO_2{}^{VI}$, VO^{IV}). The first uranium metallomesogen. crystal structure of bis(5-hexadecyloxytropolonato)copper(II). *Inorg. Chem.* **2002**, *41*, 293–299. [PubMed]
52. Motreff, A.; Correa da Costa, R.; Allouchi, H.; Duttine, M.; Mathonière, C.; Duboc, C.; Vincent, J.M. Dramatic Solid-state humidity-induced modification of the magnetic coupling in a dimeric fluorous copper(II)-carboxylate complex. *Inorg. Chem.* **2009**, *48*, 5623–5625. [CrossRef] [PubMed]
53. Volkmer, D.; Mayr, N.; Fricke, M. Crystal structure analysis of $[Ca(O_3SC_{18}H_{37})_2(DMSO)_2]$, a lamellar coordination polymer and its relevance for model studies in biomineralization. *Dalton Trans.* **2006**, 4889–4895. [CrossRef] [PubMed]
54. Pucci, D.; Barberio, G.; Crispini, A.; Francescangeli, O.; Ghedini, M.; La Deda, M. Self-organization of dipolar 4,4′-disubstituted 2,2′-bipyridine metal complexes into luminescent lamellar liquid crystals. *Eur. J. Inorg. Chem.* **2003**, *2003*, 3649–3661. [CrossRef]
55. Menger, F.M.; Lee, J.J.; Hagan, K.S. Molecular laminates. Three distinct crystal packing modes. *J. Am. Chem. Soc.* **1991**, *91*, 4017–4019. [CrossRef]
56. Zhang, W.; Zhao, F.; Liu, T.; Yuan, M.; Wang, Z.-M.; Gao, S. Spin crossover in a series of iron (II) complexes of 2-(2-alkyl-2*H*-tetrazol-5-yl)-1,10-phenanthroline: Effects of alkyl side chain, solvent, and anion. *Inorg. Chem.* **2007**, *46*, 2541–2555. [CrossRef] [PubMed]
57. Yang, Z.; Smetana, A.B.; Sorensen, C.M.; Klabunde, K.J. Synthesis and characterization of a new tiara Pd(II) thiolate complex, $[Pd(SC_{12}H_{25})_2]_6$, and its solution-phase thermolysis to prepare nearly monodisperse palladium sulfide nanoparticles. *Inorg. Chem.* **2007**, *46*, 2427–2431. [CrossRef] [PubMed]
58. Hayami, S.; Razaul Karim, M.; Lee, Y.H. Magnetic behavior and liquid-crystal properties in spin-crossover cobalt(II) compounds with long alkyl chains. *Eur. J. Inorg. Chem.* **2013**, *2013*, 683–696. [CrossRef]
59. Hayami, S.; Shigeyoshi, Y.; Akita, A.; Inoue, K.; Kato, K.; Osaka, K.; Takata, T.; Kawajiri, R.; Mitani, T.; Maeda, Y. Reverse Spin transition triggered by a structural phase transition. *Angew. Chem. Int. Ed.* **2005**, *44*, 4899–4903. [CrossRef] [PubMed]
60. Hayami, S.; Murata, K.; Urakami, D.; Kojima, Y.; Akita, A.; Inoue, K. Dynamic structural conversion in a spin-crossover cobalt (II) compound with long alkyl chains. *Chem. Commun.* **2008**, 6510–6512. [CrossRef] [PubMed]
61. Fallis, I.A.; Griffiths, P.C.; Griffiths, P.M.; Hibbs, D.E.; Hursthouse, M.B.; Winnington, A. Solid state and solution behaviour of novel transition metal containing surfactants. *Chem. Commun.* **1998**, 665–666. [CrossRef]
62. Lin, H.-C.; Huang, C.C.; Shi, C.H.; Liao, Y.H.; Chen, C.-C.; Lin, Y.-C.; Liu, Y.-H. Synthesis of alkynylated photo-luminescent Zn(II) and Mg(II) Schiff base complexes. *Dalton Trans.* **2007**, 781–791. [CrossRef] [PubMed]
63. Pietrangelo, A.; Sih, B.C.; Boden, B.N.; Wang, Z.; Li, Q.; Chou, K.C.; MacLachlan, M.J.; Wolf, M.O. Nonlinear optical properties of schiff-base-containing conductive polymer films electro-deposited in microgravity. *Adv. Mater.* **2008**, *20*, 2280–2284. [CrossRef]

64. Gandolfi, C.; Moitzi, C.; Schurtenberger, P.; Morgan, G.G.; Albrecht, M. Improved cooperativity of spin-labile iron (III) centers by self-assembly in solution. *J. Am. Chem. Soc.* **2008**, *130*, 14434–14435. [CrossRef] [PubMed]
65. Choi, H.J.; Suh, M. Nickel (II) macrocyclic complexes with long alkyl pendant chain: Synthesis, X-ray structure, and anion exchange property in the solid state. *Inorg. Chem.* **2003**, *42*, 1151–1157. [CrossRef] [PubMed]
66. Inokuchi, H.; Saito, G.; Wu, P.; Seki, K.; Tang, T.B.; Mori, M.; Imaeda, K.; Enoki, T.; Higuchi, Y.; Inaka, K.; *et al*. A novel type of organic semiconductors. molecular fastener. *Chem. Lett.* **1986**, *15*, 1263–1266. [CrossRef]
67. Neve, F. Transition metal based ionic mesogens. *Adv. Mater.* **1996**, *8*, 277–289. [CrossRef]
68. Driscoll, J.A.; Keyes, P.H.; Heeg, M.J.; Heiney, P.A.; Verani, C.N. Influence of the apical ligand in the thermotropic mesomorphism of cationic copper-based surfactants. *Inorg. Chem.* **2008**, *47*, 7225–7232. [CrossRef] [PubMed]
69. Shakya, R.; Hindo, S.S.; Wu, L.; Ni, S.; Allard, M.; Heeg, M.J.; da Rocha, S.R.P.; Yee, G.T.; Hratchian, H.P.; Verani, C.N. Amphiphilic and magnetic properties of a new class of cluster-bearing $[L_2Cu_4(\mu_4\text{-O})(\mu_2\text{-carboxylato})_4]$ soft materials. *Chem. Eur. J.* **2007**, *13*, 9948–9956. [CrossRef] [PubMed]
70. Su, P.Y.S.; Tseng, J.C.W.; Lee, K.-M.; Wang, J.-C.; Lin, I.J.B. Tetranuclear silver (I) clusters showing high ionic conductivity in a bicontinuous cubic mesophase. *Inorg. Chem.* **2012**, *51*, 98–108. [CrossRef] [PubMed]
71. Su, P.Y.S.; Hsu, S.J.; Tseng, J.C.W.; Hsu, H.-F.; Wang, W.-J.; Lin, I.J.B. Polynuclear Silver(I) Triazole Complexes: Ion Conduction and Nanowire Formation in the Mesophase. *Chem. Eur. J.* **2016**, *22*, 323–330. [CrossRef] [PubMed]
72. Ciajolo, M.R.; Corradini, P.; Pavone, V. Bis(*n*-dodecylammonium) tetrachlorozincate. *Acta Crstallogr. Sect. B* **1977**, *33*, 553–555. [CrossRef]
73. Guo, N.; Lin, Y.-H.; Zeng, G.-F.; Xi, S.-Q. Structure of 1,10-diaminodecane tetrachlorozincate. *Acta Crstallogr. Sect. C* **1992**, *48*, 650–652. [CrossRef]
74. Martin, J.D.; Keary, C.L.; Thornton, T.A.; Novotnak, M.P.; Knutson, J.W.; Folmer, J.C. Metallotropic liquid crystals formed by surfactant templating of moltenmetal halides. *Nat. Mater.* **2008**, *5*, 271–275. [CrossRef] [PubMed]
75. Lee, C.K.; Huang, H.W.; Lin, I.J.B. Simple amphiphilic liquid crystalline *N*-alkylimidazolium salts. A new solvent system providing a partially ordered environment. *Chem. Commun.* **2000**, 1911–1912. [CrossRef]
76. Lee, C.K.; Peng, H.H.; Lin, I.J.B. Liquid crystals of *N*,*N*′-dialkylimidazolium salts comprising palladium (II) and copper (II) ions. *Chem. Mater.* **2004**, *16*, 530–536. [CrossRef]
77. Wang, K.F.; Jian, F.F.; Zhuang, R.R.; Xiao, H.L. New ionic liquids of *N*,*N*′-dialkylbenzimidazolium salt comprising copper (II) ions. *Cryst. Growth Des.* **2009**, *9*, 3934–3940. [CrossRef]
78. Paulsson, H.; Berggrund, M.; Fischer, A.; Kloo, L. Iodoargentates and cuprates stabilized by sulfonium cations with long alkyl chains. *Eur. J. Inorg. Chem.* **2003**, *2003*, 2352–2355. [CrossRef]
79. Deng, F.-G.; Hu, B.; Sun, W.; Chen, J.; Xia, C.-C. Novel pyridinium based cobalt carbonyl ionic liquids: Synthesis, full characterization, crystal structure and application in catalysis. *Dalton Trans.* **2007**, 4262–4267. [CrossRef] [PubMed]
80. Oliver, S.R.J.; Lough, A.J.; Ozin, G.A. Crystal structures of a series of novel alkylammonium phosphates and their formation in aluminophosphate synthesis mixtures. *Inorg. Chem.* **1998**, *37*, 5021–5028. [CrossRef] [PubMed]
81. Li, J.; Marler, B.; Kessler, H.; Soulard, M.; Kallus, S. Synthesis, structure analysis, and characterization of a new thiostannate, $(C_{12}H_{25}NH_3)_4[Sn_2S_6]\cdot 2H_2O$. *Inorg. Chem.* **1997**, *36*, 4697–4701. [CrossRef] [PubMed]
82. Bonhomme, F.; Kanatzidis, M.G. Structurally characterized mesostructured hybrid surfactant-inorganic lamellar phases containing the adamantane $[Ge_4S_{10}]^{4-}$ anion: Synthesis and properties. *Chem. Mater.* **1998**, *10*, 1153–1159. [CrossRef]
83. Wachhold, M.; Kanatzidis, M.G. Surfactant-templated inorganic lamellar and non-lamellar hybrid phases containing adamantane $[Ge_4S_{10}]^{4-}$ anions. *Chem. Mater.* **2000**, *12*, 2914–2923. [CrossRef]
84. Rangan, K.K.; Kanatzidis, M.G. Mesolamellar thiogermanates $[C_nH_{2n+1}NH_3]_4Ge_4S_{10}$. *Inorg. Chim. Acta* **2004**, *357*, 4036–4044. [CrossRef]
85. Suh, M.-J.; Vien, V.; Huh, S.; Kim, Y.; Kim, S.-J. Mesolamellar phases containing $[Re_6Q_8(CN)_6]^{4-}$ (Q = Te, Se, S) cluster anions. *Eur. J. Inorg. Chem.* **2008**, *2008*, 686–692. [CrossRef]

86. Kind, R.; Pleško, S.; Arent, H.; Blinc, R.; Žekš, B.; Selinger, J.; Ložar, B.; Slak, J.; Levstik, A.; Filipič, C.; *et al*. Dynamics of *n*-decylammonium chains in the perovskite-type layer structure compound $(C_{10}H_{21}NH_3)_2CdCl_4$. *J. Chem. Phys.* **1979**, *71*, 2118–2130. [CrossRef]
87. Mitzi, D.B. Templating and structural engineering in organic-inorganic perovskites. *J. Chem. Soc. Dalton Trans.* **2001**, 1–12. [CrossRef]
88. Billing, D.G.; Lemmerer, A. Synthesis, characterization and phase transitions of the inorganic-organic layered perovskite-type hybrids $[(C_nH_{2n+1}NH_3)_2PbI_4]$ (n = 12, 14, 16 and 18). *New J. Chem.* **2008**, *32*, 1736–1746. [CrossRef]
89. Lemmerer, A.; Billing, D.G. Lead halide inorganic-organic hybrids incorporating diammonium cations. *CrystEngComm* **2012**, *14*, 1954–1966. [CrossRef]
90. Pradeesh, K.; Yadav, G.S.; Singh, M.; Prakash, G.V. Synthesis, structure and optical studies of inorganic-organic hybrid semiconductor, $NH_3(CH_2)_{12}NH_3PbI_4$. *Mater. Chem. Phys.* **2010**, *124*, 44–47. [CrossRef]
91. Li, J.; Bi, W.; Ki, W.; Huang, X.; Reddy, S. Nanostructured crystals: Unique hybrid semiconductors exhibiting nearly zero and tunable uniaxial thermal expansion behavior. *J. Am. Chem. Soc.* **2007**, *129*, 14140–14141. [CrossRef] [PubMed]
92. Ki, W.; Li, J. A semiconductor bulk material that emits direct white light. *J. Am. Chem. Soc.* **2008**, *130*, 8114–8115. [CrossRef] [PubMed]
93. Huang, X.; Roushan, M.; Emge, T.J.; Bi, W.; Thiagarajan, S.; Cheng, J.-H.; Yang, R.; Li, J. Flexible hybrid semiconductors with low thermal conductivity: The role of organic diamines. *Angew. Chem. Int. Ed.* **2009**, *48*, 7871–7874. [CrossRef] [PubMed]
94. Ding, N.; Armatas, G.S.; Kanatzidis, M.G. Metal inorganic frameworks: Dynamic flexible architecture with extended pore order built from $[Se_3]^{2-}$ linkers and $[Re_6Se_6Br_8]^{2-}$ clusters. *J. Am. Chem. Soc.* **2010**, *132*, 6728–6734. [CrossRef] [PubMed]
95. Kojima, A.; Teshima, K.; Shirai, Y.; Miyasaka, T. Organometal halide perovskites as visible-light sensitizers for photovoltaic cells. *J. Am. Chem. Soc.* **2009**, *131*, 6050–6051. [CrossRef] [PubMed]
96. Lee, M.M.; Teusche, J.; Miyasaka, M.; Murakami, T.N.; Snaith, H.J. Efficient hybrid solar cells based on meso-superstructured organometal halide perovskites. *Science* **2012**, *338*, 643–647. [CrossRef] [PubMed]
97. Kagan, C.R.; Mitzi, D.B.; Dimitrakopoulos, C.D. Organic-inorganic hybrid materials as semiconducting channels in thin-film field-effect transistors. *Science* **1999**, *286*, 945–947. [CrossRef] [PubMed]
98. Song, Y.-F.; Long, D.-L.; Ritchie, C.; Cronin, L. Nanoscale polyoxometalate-based inorganic/organic hybrids. *Chem. Rec.* **2011**, *11*, 158–171. [CrossRef] [PubMed]
99. Yin, P.; Li, D.; Liu, T. Solution behaviors and self-assembly of polyoxometalates as models of macroions and amphiphilic polyoxometalate-organic hybrids as novel surfactants. *Chem. Soc. Rev.* **2012**, *41*, 7368–7383. [CrossRef] [PubMed]
100. Polarz, S.; Landsmann, S.; Klaiber, A. Hybrid surfactant systems with inorganic constituents. *Angew. Chem. Int. Ed.* **2014**, *53*, 946–954. [CrossRef] [PubMed]
101. Clemente-León, M.; Coronado, E.; Soriano-Portillo, A.; Mingotaud, C.; Dominguez-Vera, J.M. Langmuir–Blodgett films based on inorganic molecular complexes with magnetic or optical properties? *Adv. Colloid Interface Sci.* **2005**, *116*, 193–203. [CrossRef] [PubMed]
102. Nisar, A.; Wang, X. Surfactant-encapsulated polyoxometalate building blocks: Controlled assembly and their catalytic properties. *Dalton Trans.* **2012**, *41*, 9832–9845. [CrossRef] [PubMed]
103. Zhang, T.; Liu, S.; Kurth, D.G.; Faul, C.F.J. Organized nanostructured complexes of polyoxometalates and surfactants that exhibit photoluminescence and electrochromism. *Adv. Funct. Mater.* **2009**, *19*, 642–652. [CrossRef]
104. Qi, W.; Wu, L. Polyoxometalate/polymer hybrid materials: Fabrication and properties. *Polym. Int.* **2009**, *58*, 1217–1225. [CrossRef]
105. Li, W.; Wu, L. Nano-hybrid liquid crystals from the self-assembly of surfactant-encapsulated polyoxometalate complexes. *Chin. J. Chem.* **2015**, *33*, 15–23. [CrossRef]
106. Ito, T. Polyoxometalate-surfactant hybrids as building strategy for two-dimensional molecular arrays. *Polyoxometalate Chem.* **2012**, *1*, 6–14.
107. Stein, A.; Fendorf, M.; Jarvie, T.P.; Mueller, K.T.; Benesi, A.J.; Mallouk, T.E. Salt-gel synthesis of porous transition-metal oxides. *Chem. Mater.* **1995**, *7*, 304–313. [CrossRef]

108. Janauer, G.G.; Dobley, A.; Guo, J.; Zavalij, P.; Whittingham, M.S. Novel tungsten, molybdenum, and vanadium oxides containing surfactant ions. *Chem. Mater.* **1996**, *8*, 2096–2101. [CrossRef]
109. Taguchi, A.; Abe, T.; Iwamoto, M. Non-silica-based mesostructured materials: Hexagonally mesostructured array of surfactant micelles and 11-tungstophosphoric heteropoly anions. *Adv. Mater.* **1998**, *10*, 667–669. [CrossRef]
110. Do, J.; Jacobson, A.J. Mesostructured lamellar phases containing six-membered vanadium borophosphate cluster anions. *Chem. Mater.* **2001**, *13*, 2436–2440. [CrossRef]
111. Zhang, G.; Ke, H.; He, T.; Xiao, D.; Chen, Z.; Yang, W.; Yao, J. Synthesis and characterization of new layered polyoxometallates-1,10-decanediamine intercalative nanocomposites. *J. Mater. Res.* **2004**, *19*, 496–500. [CrossRef]
112. Landsmann, S.; Lizandara-Pueyo, C.; Polarz, S. A new class of surfactants with multinuclear, inorganic head groups. *J. Am. Chem. Soc.* **2010**, *132*, 5315–5321. [CrossRef] [PubMed]
113. Janauer, G.G.; Dobley, A.D.; Zavalij, P.Y.; Whittingham, M.S. Evidence for decavanadate clusters in the lamellar surfactant ion phase. *Chem. Mater.* **1997**, *9*, 647–649. [CrossRef]
114. Fosse, N.; Brohan, L. Thermal and structural investigations of the bis-dihexadecyldimethylammonium dichromate. *J. Solid State Chem.* **1999**, *145*, 655–667. [CrossRef]
115. Fosse, N.; Caldes, M.; Joubert, O.; Ganne, M.; Brohan, L. Layered alkyltrimethylammonium chromates: Thermal and structural investigations and crystal structure of the anhydrous bisoctyltrimethylammonium dichromate. *J. Solid State Chem.* **1998**, *139*, 310–320. [CrossRef]
116. Spahr, M.E.; Nesper, R. Anhydrous octamolybdate with trimethyl hexadecyl ammonium cations. *Z. Anorg. Allg. Chem.* **2001**, *627*, 2133–2138. [CrossRef]
117. Ito, T.; Sawada, K.; Yamase, T. Crystal structure of bis(dimethyldioctadecylammonium) hexamolybdate: A molecular model of Langmuir-Blodgett films. *Chem. Lett.* **2003**, *32*, 938–939. [CrossRef]
118. Ito, T.; Yamase, T. Inorganic-organic hybrid layered crystal composed of polyoxomolybdate and surfactant with π electrons. *Chem. Lett.* **2009**, *38*, 370–371. [CrossRef]
119. Ito, T.; Yamase, T. Controllable layered structures in polyoxomolybdate-surfactant hybrid crystals. *Materials* **2010**, *3*, 158–164. [CrossRef]
120. Ito, T.; Mikurube, K.; Abe, Y.; Koroki, T.; Saito, M.; Iijima, J.; Naruke, H.; Ozeki, T. Hybrid inorganic-organic crystals composed of octamolybdate isomers and pyridinium surfactant. *Chem. Lett.* **2010**, *39*, 1323–1325. [CrossRef]
121. Ito, T.; Mikurube, K.; Hasegawa, K.; Kurasawa, M.; Naruke, H.; Ozeki, T. Polyoxomolybdate-surfactant hybrid layered crystal with unusually long periodicity. *Chem. Lett.* **2011**, *40*, 626–628. [CrossRef]
122. Mikurube, K.; Hasegawa, K.; Naruke, H.; Ito, T. Hybrid layered crystal comprising polyoxometalate and surfactant synthesized from reduced Mo-blue species. *J. Chem.* **2013**, *2013*, 6. [CrossRef]
123. Ito, T.; Ide, R.; Kosaka, K.; Hasegawa, S.; Mikurube, K.; Taira, M.; Naruke, H.; Koguchi, S. Polyoxomolybdate-surfactant layered crystals derived from long-tailed alkylamine and ionic-liquid. *Chem. Lett.* **2013**, *42*, 1400–1402. [CrossRef]
124. Ito, T.; Mikurube, K.; Hasegawa, K.; Matsumoto, T.; Kosaka, K.; Naruke, H.; Koguchi, S. Structural variation in polyoxomolybdate hybrid crystals comprising ionic-liquid surfactants. *Crystals* **2014**, *4*, 42–52. [CrossRef]
125. Ito, T.; Nakagawa, M.; Kobayashi, J.; Matsumoto, T.; Otobe, S.; Naruke, H. Layered and molecular-structural control in polyoxomolybdate hybrid crystals by surfactant chain length. *J. Mol. Struct.* **2016**, *1106*, 220–226. [CrossRef]
126. Ito, T.; Taira, M.; Fukumoto, K.; Yamamoto, K.; Naruke, H.; Tomita, K. Polyoxovanadate-surfactant hybrid layered crystal containing one-dimensional hydrogen-bonded cluster chain. *Bull. Chem. Soc. Jpn.* **2012**, *85*, 1222–1224. [CrossRef]
127. Ito, T.; Fujimoto, N.; Uchida, S.; Iijima, J.; Naruke, H.; Mizuno, N. Polyoxotungstate-surfactant layered crystal toward conductive inorganic-organic hybrid. *Crystals* **2012**, *2*, 362–373. [CrossRef]
128. Otobe, S.; Fujioka, N.; Hirano, T.; Ishikawa, E.; Naruke, H.; Fujio, K.; Ito, T. Decisive interactions between the heterocyclic moiety and the cluster observed in polyoxometalate-surfactant hybrid crystals. *Int. J. Mol. Sci.* **2015**, *16*, 8505–8516. [CrossRef] [PubMed]
129. Ito, T.; Mikurube, K.; Taira, M.; Yoshioka, H.; Naruke, H. Hybrid layered crystals composed of polyoxoalkoxymetalates and pyridinium surfactants. *Polyoxometalate Chem.* **2012**, *1*, 1–5.

130. Nyman, M.; Ingersoll, D.; Singh, S.; Bonhomme, F.; Alam, T.M.; Brinker, C.J.; Rodriguez, M.A. Comparative study of inorganic cluster-surfactant arrays. *Chem. Mater.* **2005**, *17*, 2885–2895. [CrossRef]
131. Nyman, M.; Rodriguez, M.A.; Anderson, T.M.; Ingersoll, D. Two structures toward understanding evolution from surfactant-polyoxometalate lamellae to surfactant-encapsulated polyoxometalates. *Cryst. Growth Des.* **2009**, *9*, 3590–3597. [CrossRef]
132. Eda, K.; Iriki, Y. Crystal engineering with $[Mo_{36}O_{112}(H_2O)_{16}]^{8-}$ anion as nanosized building block. *Chem. Lett.* **2005**, *34*, 612–613. [CrossRef]
133. Nelson, J.H.; Johnston, A.R.; Narducci Sarjeant, A.; Norquist, A.J. Composition space analysis of templated molybdates. *Solid State Sci.* **2007**, *9*, 472–484. [CrossRef]
134. Niu, Y.-Y.; Wang, L.-F.; Lv, X.R.; Du, H.-J.; Qiao, Y.-Z.; Wang, H.-M.; Song, L.-S.; Wu, B.-L.; Hou, H.-W.; Ng, S.W. Construction and isomeric transformation of polyoxometalates directed by 1,ω-bis(pyridinium)alkane templates. *CrystEngComm* **2011**, *13*, 5071–5081. [CrossRef]
135. Du, H.-J.; Mi, L.-W.; Yue, Z.-C.; Niu, Y.-Y.; Hou, H.-W. Templated fabrication, isomer recognition of series of 1,10-(alkane-1,ω-diyl)-bis(3-methylimidazolium)-induced polyoxometalates (ω = 1–11). *Inorg. Chim. Acta* **2014**, *409*, 418–426. [CrossRef]
136. Yue, Z.-C.; Du, H.-J.; Li, L.; Zhang, W.-L.; Niu, Y.-Y.; Hou, H.-W. Construction and isomer recognition of polyoxometalates functionalized by 1,2-dimethylimidazole alkane templates. *Inorg. Chim. Acta* **2014**, *410*, 136–143. [CrossRef]
137. Yin, P.; Wu, P.; Xiao, Z.; Li, D.; Bitterlich, E.; Zhang, J.; Cheng, P.; Vezenov, D.V.; Liu, T.; Wei, Y. A double-tailed fluorescent surfactant with a hexavanadate cluster as the head group. *Angew. Chem. Int. Ed.* **2011**, *50*, 2521–2525. [CrossRef] [PubMed]
138. Yin, P.; Bayaguud, A.; Cheng, P.; Haso, F.; Hu, L.; Wang, J.; Vezenov, D.; Winans, R.E.; Hao, J.; Tao, L.; *et al.* Spontaneous stepwise self-assembly of a polyoxometalate-organic hybrid into catalytically active one-dimensional anisotropic structures. *Chem. Eur. J.* **2014**, *20*, 9589–9595. [CrossRef] [PubMed]
139. Zhu, L.; Chen, K.; Hao, J.; Wei, Z.; Zhang, H.; Yin, P.; Wei, Y. Synthesis and crystallization behavior of surfactants with hexamolybdate as the polar headgroup. *Inorg. Chem.* **2015**, *54*, 6075–6077. [CrossRef] [PubMed]
140. Song, Y.-F.; McMillan, N.; Long, D.-L.; Thiel, J.; Ding, Y.; Chen, H.; Gadegaard, N.; Cronin, L. Design of hydrophobic polyoxometalate hybrid assemblies beyond surfactant encapsulation. *Chem. Eur. J.* **2008**, *14*, 2349–2354. [CrossRef] [PubMed]
141. Zhang, J.; Li, W.; Wu, C.; Li, B.; Zhang, J.; Wu, L. Redox-controlled helical self-assembly of a polyoxometalate complex. *Chem. Eur. J.* **2013**, *19*, 8129–8135. [CrossRef] [PubMed]
142. Strong, J.B.; Ostrander, R.; Rheingold, A.L.; Maatta, E.A. Ensheathing a Polyoxometalate: Convenient Systematic Introduction of Organoimido Ligands at Terminal Oxo Sites in $[Mo_6O_{19}]^{2-}$. *J. Am. Chem. Soc.* **1994**, *116*, 3601–3602. [CrossRef]
143. Favette, S.; Hasenknopf, B.; Vaissermann, J.; Gouzerh, P.; Roux, C. Assembly of a polyoxometalate into an anisotropic gel. *Chem. Commun.* **2003**, 2664–2665. [CrossRef]
144. Chambers, R.C.; Atkinson, E.J.O.; McAdams, D.; Hayden, E.J.; Brown, A.J.A. Creating monolayers and thin films of a novel bis(alkyl) substituted asymmetrical polyoxotungstate, $\{[CH_3(CH_2)_{11}Si]_2OSiW_{11}O_{39}\}^{4-}$ using the Langmuir-Blodgett technique. *Chem. Commun.* **2003**, 2456–2457. [CrossRef]
145. Zhang, J.; Song, Y.-F.; Cronin, L.; Liu, T. Self-assembly of organic-inorganic hybrid amphiphilic surfactants with large polyoxometalates as polar head groups. *J. Am. Chem. Soc.* **2008**, *130*, 14408–14409. [CrossRef] [PubMed]
146. Han, Y.; Xiao, Y.; Zhang, Z.; Liu, B.; Zheng, P.; He, S.; Wang, W. Synthesis of polyoxometalate-polymer hybrid polymers and their hybrid vesicular assembly. *Macromolecules* **2009**, *42*, 6543–6548. [CrossRef]
147. Landsmann, S.; Luka, M.; Polarz, S. Bolaform surfactants with polyoxometalate head groups and their assembly into ultra-small monolayer membrane vesicles. *Nat. Comm.* **2012**, *3*, 1299. [CrossRef] [PubMed]
148. Jallet, V.; Guillemot, G.; Lai, J.; Bauduin, P.; Nardello-Rataj, V.; Proust, A. Covalent amphiphilic polyoxometalates for the design of biphasic microemulsion systems. *Chem. Commun.* **2014**, *50*, 6610–6612. [CrossRef] [PubMed]
149. Lesage de La Haye, J.; Guigner, J.-M.; Marceau, E.; Ruhlmann, L.; Hasenknopf, B.; Lacôte, E.; Rieger, J. Amphiphilic polyoxometalates for the controlled synthesis of hybrid polystyrene particles with surface reactivity. *Chem. Eur. J.* **2015**, *21*, 2948–2953. [CrossRef] [PubMed]

150. Bu, W.; Li, W.; Li, H.; Wu, L.; Tang, A.-C. Surfactant-encapsulated polyoxometalloeuropate: Polarized Eu^{3+} emission in the highly ordered self-organizing film. *J. Colloid Interaface Sci.* **2004**, *274*, 200–203. [CrossRef] [PubMed]
151. Chang, H.-C.; Kiriya, D. Synchronic transformations of molecular states and macroscopic phases in valence-tautomeric complexes. *Eur. J. Inorg. Chem.* **2013**, *2013*, 642–652. [CrossRef]
152. Kitchen, J.A.; White, N.G.; Jameson, G.N.L.; Tallon, J.L.; Brooker, S. Effect of counteranion X on the spin crossover properties of a family of diiron(II) triazole complexes $[Fe^{II}{}_2(PMAT)_2](X)_4$. *Inorg. Chem.* **2011**, *50*, 4586–4597. [CrossRef] [PubMed]
153. Bünzli, J.-C.G. Benefiting from the unique properties of lanthanide ions. *Acc. Chem. Res.* **2006**, *39*, 53–61. [CrossRef] [PubMed]
154. Binnemans, K. Lanthanide-based luminescent hybrid materials. *Chem. Rev.* **2009**, *109*, 4283–4374. [CrossRef] [PubMed]
155. Kitchen, J.A.; Barry, D.A.; Mercs, L.; Albrecht, M.; Peacock, R.D.; Gunnlaugsson, T. Circularly polarized lanthanide luminescence from Langmuir-Blodgett films formed from optically active and amphiphilic Eu^{III} based self-assembly complexes. *Angw. Chem. Int. Ed.* **2012**, *51*, 704–708. [CrossRef] [PubMed]
156. Osaka, I.; Takimiya, K. Backbone orientation in semiconducting polymers. *Polymer* **2015**, *59*, A1–A15. [CrossRef]
157. Wang, C.; Gu, P.; Hu, B.; Zhang, Q. Recent progress in organic resistance memory with small molecules and inorganic-organic hybrid polymers as active elements. *J. Mater. Chem. C* **2015**, *3*, 10055–10065. [CrossRef]
158. Douvas, A.M.; Makarona, E.; Glezos, N.; Argitis, P.; Mielczarski, J.A.; Mielczarski, E. Polyoxometalate-based layered structures for charge transport control in molecular devices. *ACS Nano* **2008**, *2*, 733–742. [CrossRef] [PubMed]